Light-Induced Dynamics in Photosystem I Electron Transfer

Shana L. Bender and Bridgette A. Barry
School of Chemistry and Biochemistry, Georgia Institute of Technology and the Petit Institute of Bioengineering and Bioscience, Atlanta, Georgia 30332

ABSTRACT Protein dynamics are likely to play important, regulatory roles in many aspects of photosynthetic electron transfer, but a detailed description of these coupled protein conformational changes has been unavailable. In oxygenic photosynthesis, photosystem I catalyzes the light-driven oxidation of plastocyanin or cytochrome *c* and the reduction of ferredoxin. A chlorophyll (chl) *a*/*a*′ heterodimer, P_{700}, is the secondary electron donor, and the two P_{700} chl, are designated P_A and P_B. We used specific chl isotopic labeling and reaction-induced Fourier-transform infrared spectroscopy to assign chl keto vibrational bands to P_A and P_B. In the cyanobacterium, *Synechocystis* sp. PCC 6803, the chl keto carbon was labeled from ^{13}C-labeled glutamate, and the chl keto oxygen was labeled from $^{18}O_2$. These isotope-based assignments provide new information concerning the structure of P_A^+, which is found to give rise to two chl keto vibrational bands, with frequencies at 1653 and 1687 cm^{-1}. In contrast, P_A gives rise to one chl keto band at 1638 cm^{-1}. The observation of two P_A^+ keto frequencies is consistent with a protein relaxation-induced distribution in P_A^+ hydrogen bonding. These results suggest a light-induced conformational change in photosystem I, which may regulate the oxidation of soluble electron donors and other electron-transfer reactions. This study provides unique information concerning the role of protein dynamics in oxygenic photosynthesis.

INTRODUCTION

In oxygenic photosynthesis, photosystem I (PSI) is a multi-subunit, membrane-protein complex, which carries out the light-induced reduction of ferredoxin and the oxidation of plastocyanin or cytochrome *c* (1). These redox events are initiated by light-induced electron transfer, leading to the oxidation of a chlorophyll (chl) dimer, P_{700}, and the reduction of an iron-sulfur cluster, F_B (2,3). Other electron-transfer cofactors include the primary chl donor (eC-2 or eC-3), two A_0 chl and two A_1 phylloquinone electron acceptors, and two additional iron-sulfur clusters, F_X and F_A. The PSI reaction center contains two large intrinsic polypeptides, PsaA and PsaB (3). The 2.5-Å crystal structure reveals a pseudo-C_2 symmetric arrangement of the accessory chl molecules and of the two A_0 and the two A_1 electron acceptors. These two branches of electron-transfer cofactors are referred to as the PsaA and PsaB branches (3). Studies suggest that both branches carry out light-induced electron transfer (4,5).

Recent studies suggest that charge separation begins on an accessory chl monomer (either eC-2 or eC-3) that donates its electron to an A_0 acceptor (6). This primary donor is reduced by P_{700}, a chl *a*/*a*′ heterodimer, which is the terminal electron donor in the PSI reaction center (7). The heterodimer P_{700} is present in the dark, and P_{700}^+ is produced under illumination. The heterodimer P_{700} consists of a chl *a* molecule, designated P_B, and a chl *a*′ molecule, designated P_A. Although the x-ray structure supports the interpretation that P_A has hydrogen-bonding interactions with its protein environment, P_B does not appear to be hydrogen-bonded (3,8).

The soluble copper-containing protein, plastocyanin, acts as the electron donor to P_{700}^+ in plants, algae, and cyanobacteria. Under copper-limiting conditions, cytochrome *c* can replace plastocyanin as the electron donor in cyanobacteria (9). In plants and algae, plastocyanin docks with the luminal side of PSI to form an interaction complex, in which electron transfer from the reduced copper to P_{700}^+ occurs on the microsecond timescale (10,11). In cyanobacteria, the cytochrome, but not plastocyanin, was proposed to form an electron-transfer complex in vivo (12). In both cyanobacteria and algae, mutations in a hydrophobic region near P_{700}^+, which contains luminal PsaA and PsaB helices and a conserved tryptophan dimer, disrupt electron transfer (13–15). It was proposed that conformational rearrangements may regulate electron transfer in the interaction complex (10,16); however, see Drepper et al. for another view (17).

Previously, site-directed mutagenesis and various spectroscopic techniques were used to study the interaction of the cation radical, P_{700}^+, with its protein environment (2, 7,8,18,19). Electron paramagnetic resonance spectroscopy studies concluded that the unpaired spin is localized mainly on P_B, whereas Fourier-transform infrared spectroscopy (FT-IR) studies concluded that the spin-density is evenly distributed over the dimer (20,21). This discrepancy may be related to unsolved questions concerning the assignment of FT-IR vibrational bands, as described below.

Recent experimental (22) and previous theoretical (23–25) studies have underscored the role of protein dynamics in the control of primary electron transfer in the bacterial reaction center. In the chl-containing reaction center, photosystem II, an influence of protein dynamics on the photosynthetic

Submitted April 16, 2008, and accepted for publication June 23, 2008.

Address reprint requests to Bridgette A. Barry, School of Chemistry and Biochemistry, Georgia Institute of Technology and the Petit Institute of Bioengineering and Bioscience, Atlanta, GA 30332. Tel.: 404-385-6085; Fax: 404-894-2295; E-mail: bridgette.barry@chemistry.gatech.edu.

Editor: Michael Edidin.

0006-3495/08/10/3927/08 $2.00

doi: 10.1529/biophysj.108.135418

water-splitting cycle was also suggested by vibrational spectroscopic experiments on different timescales (26–28). In PSI, conformational dynamics have the potential to regulate the bidirectionality of electron transfer in the reaction center, as well as the mechanism of plastocyanin/cytochrome *c* oxidation. The effect of light-induced dynamics on P_{700} and P_{700}^{+} can be detected in real time using vibrational spectroscopic techniques, such as FT-IR spectroscopy. Previously, evidence for structural heterogeneity in P_{700}/P_{700}^{+} was obtained by methyl ester-labeling of chl (29).

The light-minus-dark, P_{700}^{+}-minus-P_{700}, FT-IR spectrum is dominated by keto vibrational bands from chl and chl^{+}, which, in model compounds, are upshifted in frequency by oxidation (20,30,31). Keto vibrational frequencies are expected to reflect changes in polarity, hydrogen bonding, and electrostatics (32). Previously, keto vibrational bands were assigned to P_A, P_A^{+}, P_B, and P_B^{+} in the P_{700}^{+}-minus-P_{700} spectrum. The observation of four keto vibrational bands was attributed to the oxidation-induced change in the force constant, as well as differences in hydrogen-bonding interactions between the two halves of the dimer, P_A and P_B (20,31,33–35). However, there is also controversy over the assignment of the keto FT-IR bands of P_{700} and P_{700}^{+} (20,31), and the spectrum still contains unassigned bands. Therefore, the development of specific methods to isotopically label chl, with minimal interference from protein labeling, is of particular importance.

We describe methods to ^{13}C-label and ^{18}O-label the chl keto position (Fig. 1) through manipulation of the cyanobacterial chl biosynthetic pathway (36,37). These isotopically labeled samples were used to assign the 13^1-keto stretching bands of the P_{700}^{+}-minus-P_{700} FT-IR spectrum. These data reveal unexpected cofactor-protein relaxation events, which accompany light-induced electron transfer in PSI.

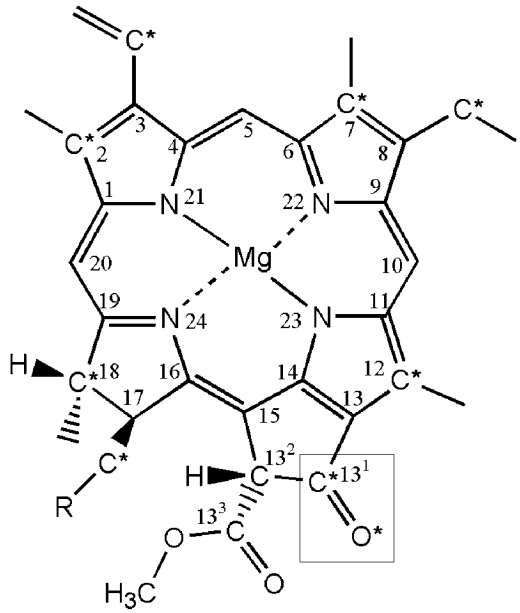

FIGURE 1 Structure of chlorophyll *a* displays the eight carbons (*asterisks*) that will be isotopically labeled from glutamic-^{13}C-3 acid. The keto group of chl is boxed. The keto oxygen (*asterisk*) will be isotopically labeled from $^{18}O_2$.

MATERIALS AND METHODS

For ^{13}C chl labeling, glutamate-tolerant *Synechocystis* PCC 6803 cultures were grown on solid media containing BG-11 (57), 250 μM L-glutamic acid buffered with 1 mM TES-NaOH, pH 8.0, 5 mM TES-NaOH, pH 8.0, and 6 mM $Na_2S_2O_3$ (39). Liquid cultures (400 mL) were grown in BG-11, 5 mM TES-NaOH, pH 8.0, and 5 μg/mL kanamycin, and were bubbled with sterile air. Cultures were supplemented with 1 mM L-glutamic acid or L-glutamic-3-^{13}C acid (99% enrichment, Isotec, Miamisburg, OH), which were buffered with 1 mM TES-NaOH, pH 8.0. Cultures were harvested at an OD_{730} (optical density) nm of 1.1–1.4.

For ^{18}O chl labeling, *Synechocystis* PCC 6803 cultures were grown on solid media containing BG-11, 5 mM TES-NaOH, pH 8.0, 6 mM $Na_2S_2O_3$, and 5 mM glucose. Liquid cultures were grown as described above, except that cultures were continuously shaken on a cell-culture agitator (New Brunswick Scientific, Edison, NJ). Carbon dioxide was bubbled into the cell cultures at a rate of 1 mL/min for 5 min daily. Immediately afterward, $^{16}O_2$ or $^{18}O_2$ (99% enrichment, Isotec) was bubbled into the cell cultures at a rate of 1 mL/min for 5 min. Cultures were grown for a total of 10 days. The OD_{730} for the cultures ranged from 1.0–1.1.

Trimeric PSI was purified, and FT-IR spectroscopy was performed as previously described (29,40–43), and as outlined in the Supplementary Material (Data S1). Evaluation of signal-to-noise in the FT-IR experiment was performed as described in the Supplementary Material (Data S1).

RESULTS

To label the oxygen of the 13^1 chl keto group, *Synechocystis* sp. PCC 6803 cyanobacterial cultures were grown in the presence of $^{18}O_2$. The formation of the chl *a* isocyclic ring is an aerobic process, in which the 13^1 oxo group (Fig. 1) is derived from molecular oxygen, using an oxygenase (44–48). The amount of ^{18}O labeling was measured by mass spectrometry, and was found to be 15% ± 6% (Fig. 2 *A*, and the Supplementary Material, Data S1). The keto position of chl (Fig. 1) constitutes the only group that is labeled by this protocol (44–47).

Reaction-induced FT-IR spectra were acquired from control and ^{18}O-labeled PSI samples (Fig. S1 in the Supplementary Material, Data S1). The difference spectra, constructed by the subtraction of data recorded under illumination and in the dark, are attributable to $P_{700}^{+}F_B^{-}$-minus-$P_{700}F_B$ (20,43). The region of the isotope-edited spectrum presented in Fig. 3 *A* exhibits keto-stretching contributions from P_{700} (negative) and P_{700}^{+} (positive) (18,20,30,31). Spectral changes associated with the labeling of chl keto oxygen can be identified by an interactive subtraction of control and ^{18}O-labeled data. This interactive subtraction minimizes any small contributions from the chl ester 1754(+)/1749(−) cm^{-1} bands (29). Small differences in amplitude in this region can arise from minor alterations in the amount of stable charge separation (Fig. S1 in the Supplementary Material, Data S1). The resulting isotope-edited spectrum (Fig. 3 *A*) will have contributions only

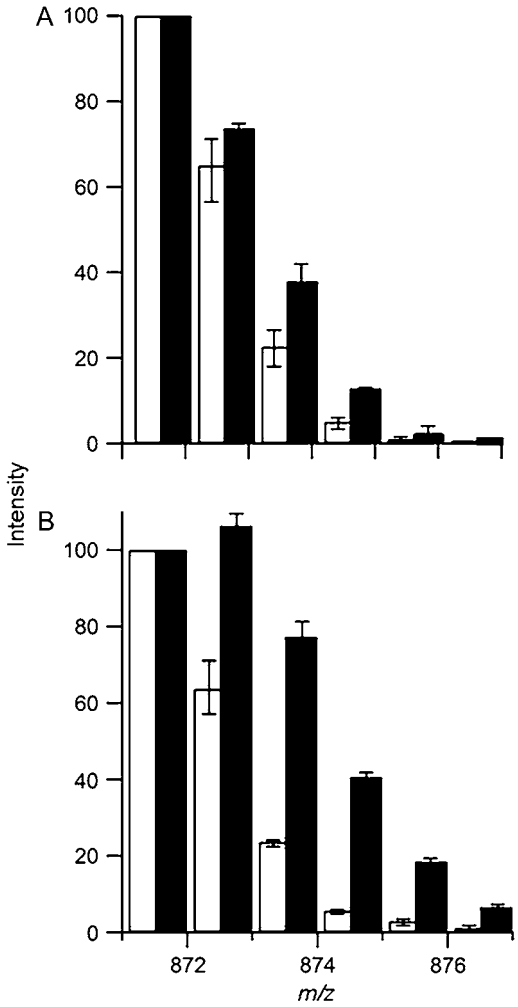

FIGURE 2 Matrix-assisted laser desorption ionization (MALDI) mass spectrometry shows incorporation of ^{18}O and ^{13}C into cyanobacterial chl. (*A*) Cyanobacteria were cultured in the presence of $^{16}O_2$ (*open columns*) or $^{18}O_2$ (*solid columns*). (*B*) Cyanobacteria were cultured in the presence of natural-abundance glutamic acid (*open columns*) or L-glutamic-3-^{13}C-acid (*solid columns*). The normalized 871.5 *m/z* peak corresponds to the [M + H] ion of pheophytin, which was generated by acid treatment of the chl sample immediately before the measurement. See the Supplementary Material (Data S1) and Materials and Methods for additional information.

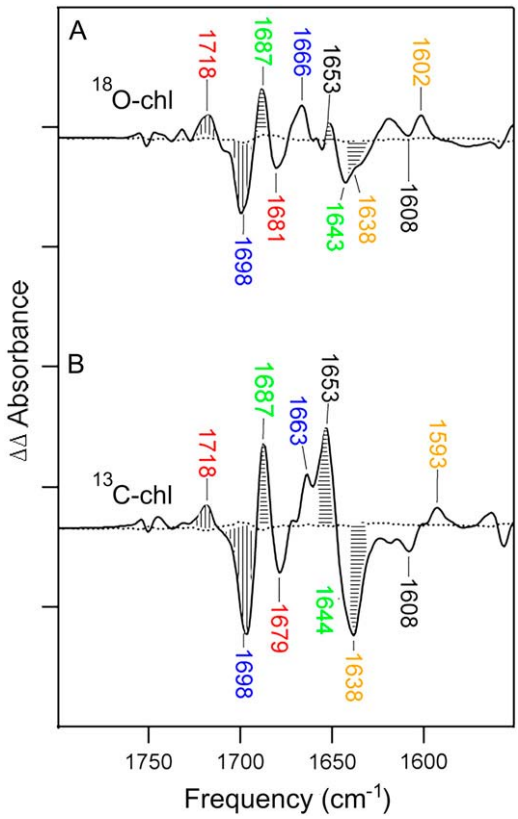

FIGURE 3 Isotope-edited FT-IR spectra show effects of ^{18}O and ^{13}C chl labeling on P^+_{700}/P_{700} keto vibrational bands. (*A*) ^{16}O-minus-^{18}O spectrum. (*B*) ^{12}C-minus-^{13}C spectrum. In *A* and *B*, control difference spectra, in which no vibrational bands are expected, are also presented as dotted lines. Natural-abundance bands assigned to P_B and P^+_B are shaded with vertical lines. Natural-abundance bands assigned to P_A and P^+_A are shaded with horizontal lines. The natural-abundance band (*solid*) and its corresponding isotope-shifted component (*open*) are labeled with the same color. (*A*) Sixty-nine spectra were averaged. (*B*) Sixty-four spectra were averaged. In *A* and *B*, the sample size was 64 μg chl. Each tick mark represents 5×10^{-4} absorbance units. See the Supplementary Material (Data S1) and Materials and Methods for additional information.

from vibrational bands perturbed by P_{700} oxidation, and by the incorporation of the ^{18}O isotope at the keto position. In the isotope-edited spectrum, natural-abundance P_{700} bands are negative, and natural-abundance P^+_{700} bands are positive. The isotope-shifted components for each vibrational band have the opposite sign. Observed spectral features in Fig. 3 *A* are significant compared with the noise, which is estimated from a control-minus-control spectrum (Fig. 3 *A*, *dotted line*).

To interpret the ^{18}O isotope-edited spectrum, the incorporation of ^{13}C at the 13^1 carbon (Fig. 1) is advantageous, because $13^1/^{13}C$ labeling will also shift spectral bands assignable to the keto-stretching vibration. In cyanobacterial chl biosynthesis, aminolevulinic acid, the first universal tetrapyrrole precursor, is formed from glutamate, which is activated by ligation to a tRNA molecule (49–53). In our experiments, carbon-labeling at the chl 13^1 position was accomplished by the growth of a glutamate-tolerant strain of *Synechocystis* sp. PCC 6803 in the presence of 1 mM glutamate, which was ^{13}C-labeled at the third carbon (Table S1 in the Supplementary Material, Data S1). Uptake of this isotope is expected to label the 13^1 carbon of chl (Fig. 1) and seven other chl carbons (Fig. 1) (36). The vibrational bands, which are altered by labeling at nonketo positions, are expected to be distinct in frequency from the keto vibrational bands (54). Furthermore, only a keto vibrational band will be shifted by both ^{18}O and $13^1/^{13}C$ labeling, and CO vibrational bands will be in common between the two types of isotope-edited spectra. Gas chromatography-mass spectral analysis of hydrolyzed PSI demonstrated that there was little scrambling of the ^{13}C glutamate label into other amino acids (Table S2 in the Supplementary Material, Data S1 (55)). Mass spectrom-

etry (Fig. 2 *B*, and Table S1, Data S1) revealed that singly, doubly, and triply ^{13}C-labeled chl isotopomers were generated at a significant yield (78%). For example, the yield of the $^{+}1$, $^{+}2$, and $^{+}3$ ^{13}C isotopomers was determined to be 43% ± 8%, 27% ± 7%, and 8% ± 5%, respectively. Only 2% ± 4% of the $^{+}4$ isotopomer was detected (Table S2, Data S1). Using these measured values, the total probability of labeling at the keto carbon position can be estimated as 16% (Table S1, Data S1). The NMR spectroscopy of purified, extracted ^{13}C-labeled chl in organic solvents (56) confirmed the incorporation of label into the keto position (data not shown).

Reaction-induced FT-IR spectra were acquired from these ^{13}C-labeled PSI samples. The solid line in Fig. 3 *B* is the ^{13}C isotope-edited spectrum, which exhibits significant features relative to the noise (Fig. 3 *B*, *dotted line*), and was produced from an interactive subtraction (Supplementary Material, Data S1). In Fig. 3, related natural-abundance and isotopomer keto bands, which are expected to be of opposite signs, are labeled with the same color code. Bands assigned to natural-abundance P_B and P_B^+ are indicated by vertical lines, and bands assigned to natural abundance P_A and P_A^+ are indicated by horizontal lines (Fig. 3). The assignment of bands in the ^{18}O and ^{13}C isotope-edited spectra is summarized in Table 1.

Bands at (+) 1718 and (−) 1698 cm^{-1} are observed in Fig. 3, *A* and *B*, consistent with assignment to a chl keto vibrational band, which is upshifted by light-induced electron transfer. Based on the signs, the positive 1718 cm^{-1} band would be assignable to P_{700}^+, and the negative 1698 cm^{-1} band would be assignable to P_{700}. For these bands, an isolated, CO harmonic-oscillator approximation predicts frequency downshifts of ~40 cm^{-1} with either ^{13}C or ^{18}O labeling. The isotope-shifted components for the (+) 1718 cm^{-1} band are observed at (−) 1681 cm^{-1} in the ^{18}O-labeled samples (Fig. 3 *A*, *red labels*) and (−) 1679 cm^{-1} in the ^{13}C-labeled samples (Fig. 3 *B*, *red labels*), respectively. The isotope-shifted components for the (−) 1698 cm^{-1} band are observed at (+) 1666 cm^{-1} in the ^{18}O-labeled (Fig. 3 *A*, *blue labels*) and (+) 1663 cm^{-1} in the ^{13}C-labeled (Fig. 3 *B*, *blue labels*) samples, respectively. Therefore, the derived ^{13}C and ^{18}O isotope shifts for the 1718 cm^{-1} and 1698 cm^{-1} bands are 37–39 cm^{-1} and 32–35 cm^{-1} (Fig. 3), respectively, in reasonable agreement with the harmonic-oscillator predictions for an isolated CO vibrational mode. In previous studies, spectral features at (+) 1717 cm^{-1} and (−) 1698 cm^{-1} were assigned to the nonhydrogen-bonded keto band of P_B^+ and P_B, respectively (20,31), and our isotope-based assignments are in agreement with those previous findings.

Bands at (+) 1653 and (−) 1638 cm^{-1} are observed in Fig. 3, *A* and *B*, consistent with assignment to a chl keto vibrational band that is perturbed by light-induced electron transfer. Based on the signs, the positive 1653 cm^{-1} band would be assignable to P_{700}^+, and the negative 1638 cm^{-1} band would be assignable to P_{700}. For these bands, the harmonic-oscillator approximation predicts frequency downshifts of ~40 cm^{-1}. The isotope-shifted components for the (+) 1653 cm^{-1} band are observed at (−) 1608 cm^{-1} (Fig. 3, *A* and *B*, *black labels*). The isotope-shifted components for the (−) 1638 cm^{-1} band are observed at (+) 1602 cm^{-1} (Fig. 3 *A*, *orange labels*) and (+) 1593 cm^{-1} (Fig. 3 *B*, *orange labels*). Therefore, the derived ^{13}C and ^{18}O isotope shifts for the (+) 1653 cm^{-1} and (−) 1638 cm^{-1} bands are 45 cm^{-1} and 36–45 cm^{-1}, respectively, in reasonable agreement with harmonic-oscillator predictions. In previous studies, spectral features at (+) 1653/4 and (−) 1638 cm^{-1} were assigned to hydrogen-bonded keto bands of P_A^+ and P_A, respectively (20,31), and our isotope-labeling work is consistent with those assignments.

Based on model compounds (30), P_A, P_A^+, P_B, and P_B^+ would be expected to give rise to one chl keto vibrational band each. Four keto bands with distinct frequencies are assigned in Table 1, based on the arguments described above. However, in each of the isotope-edited spectra presented in Fig. 3, *A* and *B*, there is still an unassigned positive band at 1687 cm^{-1}, and an unassigned negative band at 1644/3 cm^{-1} (*green labels*). If the 1687 cm^{-1} band arises from a chl keto vibration, harmonic-oscillator treatment predicts a frequency of 1645 cm^{-1} and 1648 cm^{-1} for the ^{18}O and ^{13}C isotopically labeled vibrational band, respectively. This comparison supports the interpretation that the positive 1687 cm^{-1} band is a keto vibrational band of P_{700}^+, and that the 1644/3 cm^{-1} band is its isotope-shifted component. Therefore, we assign the 1687 cm^{-1} spectral feature to a second keto vibrational band of P_B^+ or P_A^+. Based on previous site-directed mutagenesis work, we favor the assignment of this band to P_A^+ (see Discussion). The observation of two bands for P_A^+, one at 1687 cm^{-1} and the other at 1653 cm^{-1}, and of one band for P_A at 1638 cm^{-1}, suggests that light-induced electron transfer leads to a structural change in the PSI reaction center. This structural change results in at least two distinct protein environments for the P_A half of the P_{700} dimer.

TABLE 1 Chlorophyll keto assignments for P_A and P_B in photosystem I

Natural abundance*	^{18}O keto-labeled*	^{13}C keto-labeled*	Assignment
1718	1681	1679	P_B^+
1698	1666	1663	P_B
1687	1643	1644	P_A^+
1653	1608	1608	P_A^+
1638	1602	1593	P_A

*Frequencies are in wave numbers (cm^{-1}).

DISCUSSION

We incorporated ^{13}C and ^{18}O isotopic labels specifically into the chl 13^1 keto group. Cyanobacterial cultures were used, and ^{13}C glutamate and $^{18}O_2$ constituted the source of the two labels. The amount of labeling at the keto position was found

to be 15–16%, which is sufficient for detection using FT-IR spectroscopy. In addition, chl labeling occurred with minimal scrambling into amino-acid biosynthetic pathways.

Fig. 4 *A* shows the amino acids within 4 Å of the 13^1 keto group of P_A and P_B (3). Ring V of P_A is not planar with the rest of molecule, and the 13^1 keto group of P_A is predicted to participate in a hydrogen bond with a conserved threonine residue, Thr-743 (*Synechococcus elongatus* numbering). There are no analogous hydrogen bonds predicted on the P_B half of the P_{700} dimer (Fig. 4 *A*). Therefore, the keto vibrational bands of P_A/P_A^+ should be distinguishable from P_B/P_B^+ bands. Previous assignments of 13^1 keto stretching vibrations of P_B, P_A, P_B^+, and P_A^+ were based on mutagenesis studies, global ^2H incorporation, global ^{15}N incorporation, and comparisons to model compounds (20,30,31). These approaches led to some discrepancies in the interpretation of the PSI difference spectrum. Specific isotopic labeling, as performed here, has clarified the assignments. Four of our isotope-based P_B, P_B^+, P_A, and P_A^+ assignments are consistent with previous findings (Table 1). However, we have identified an additional positive band at 1687 cm^{-1}, which is a chl keto vibration, based on its ^{13}C and ^{18}O isotope-induced downshifts. The sign of this band indicates that it arises from P_B^+ or P_A^+. This positive band was observed previously in wild-type PSI (20,30), and was either unassigned or assigned to a P_A^+ keto vibration, which was rationalized to downshift from 1695 cm^{-1} with oxidation (31). However, model compound studies predict an oxidation-induced upshift (20,30).

We favor the assignment of the 1687 cm^{-1} spectral band to the chl keto vibrational band of P_A^+, which upshifts from 1638 cm^{-1} with light-induced oxidation. This interpretation is consistent with previous site-directed mutagenesis studies. In that previous work, mutations at the conserved threonine were used to disrupt the hydrogen-bonding network of P_A, and an increase in the amplitude of a positive 1687 cm^{-1} band was observed (33–35). This increase in amplitude was attributed to an increased population of a more weakly hydrogen-bonded P_A^+ in the mutant (33). However, there was no significant change in amplitude of the 1687 cm^{-1} band when mutations were used to introduce hydrogen bonds to P_B (57).

Based on these previous investigations, we suggest that the 1687-cm^{-1} band arises from a state in which the P_A^+ hydrogen-bond to Thr is weakened by a light-induced protein structural change. In this interpretation, there are two populations of P_A^+, which are generated under illumination: a strongly hydrogen-bonded version, which contributes to the 1653 cm^{-1} band, and a less strongly hydrogen-bonded version, which contributes to the difference spectrum at 1687 cm^{-1}. Our observation of only one P_A chl keto band, at 1638 cm^{-1}, demonstrates that the conformational change is light-induced. Thus, our findings suggest a light-induced protein relaxation event that weakens the hydrogen bond between P_A and Thr, most likely by a change in distance or angle between the 13^1 keto group of P_A and the Thr side chain. To explain our observation of the 1653 cm^{-1} band, this change in hydrogen-bonding must occur in only a subset of PSI reaction centers.

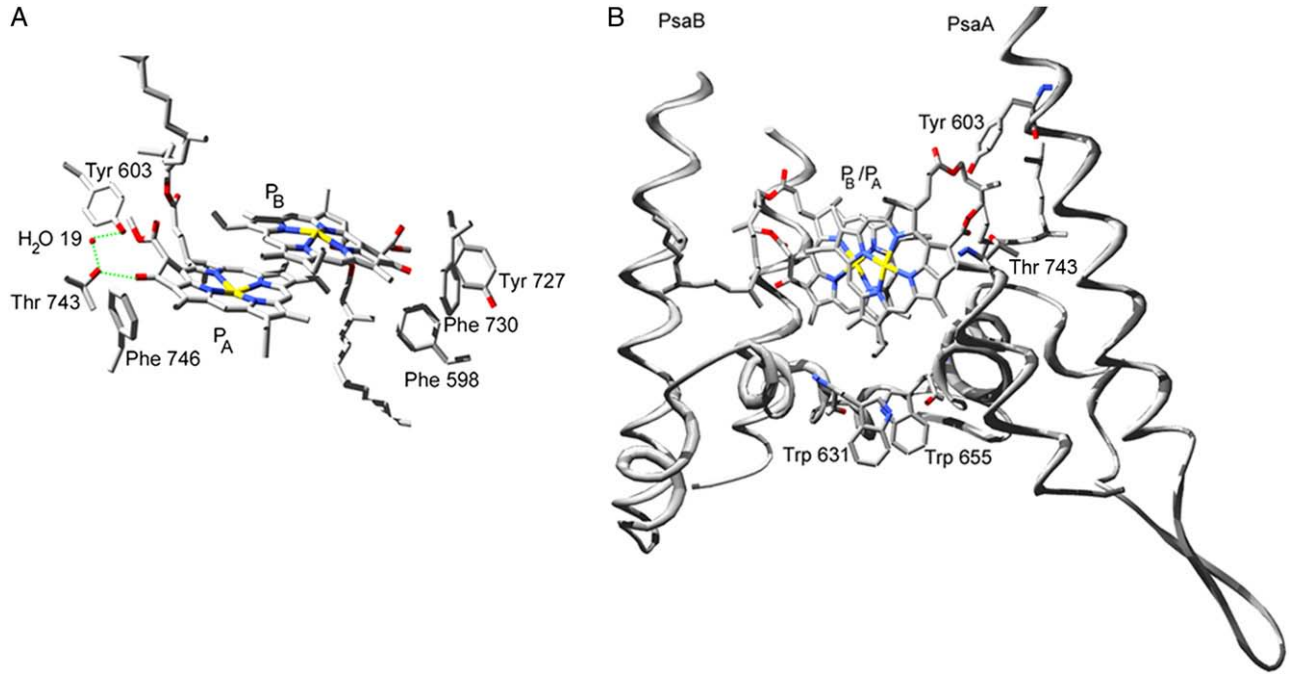

FIGURE 4 (*A*) Protein environment of P_A and P_B in P_{700}. The hydrogen-bonding network of P_A with Thr-743, H_2O, and Tyr-603 is represented by dashes. (*B*) Luminal helices of PsaB and PsaA near P_{700}. This visualization is reproduced from the 2.5-Å crystal structure of PSI from *S. elongatus* (Protein Data Bank file accession number 1JB0 (3)), using the Swiss-PDB viewer (version 3.7; www.expasy.ch/spdbc), with numbering according to *S. elongatus*, and rendered using POV-Ray (version 3.5; www.povray.org).

In our experiments, PSI vibrational spectra were recorded under continuous, low-intensity, red-filtered illumination. The data-acquisition time was 4 min. In PSI, forward electron transfer from the primary donor to the terminal electron acceptor, F_B, occurs with a time constant of ~500 ns, and $P_{700}^+F_B^-$ recombination events occur on a timescale of tens of milliseconds (2). Therefore, our experiment is expected to generate a photosteady state. In this photosteady state, protein-relaxation events, which are coupled to the initial charge separation, will have the opportunity to accumulate under illumination, and to influence the spectrum of P_{700}^+.

In our previous chl ester-labeling experiments, P_{700}^+/P_{700} (29) was demonstrated to have more than four ester frequencies. Multiple, distributed ester frequencies are likely to be caused by the protein structural changes under discussion here. It was suggested that these multiple ester frequencies could reflect a distribution in keto-enol tautomerization. Such a structural change is expected to be coupled with alterations in hydrogen-bonding, which will also alter the double-bond character in the isocyclic ring of P_A (29). Comparison with this previous study suggests that both keto and ester vibrational bands can be used as reporters for light-induced protein-relaxation events in PSI.

In PSI, two rates are observed for oxidation of A_1^- by F_X, which were attributed to oxidation of the A_{1A}^- and A_{1B}^- species (4,5). The rates of the two processes are ~200 ns and 20 ns, although the relative amplitudes of the two kinetic phases differ in different organisms (2,58,59). In the bacterial reaction center, however, electron transfer to the intermediate acceptor, bacteriopheophytin, is unidirectional in wild-type preparations (60,61). Our observation of a P_A side structural change raises the question of whether this protein-relaxation event alters the rates and amplitudes of the A and B side electron transfer. Based on mutation studies, the midpoint potential of P_{700} was previously found to decrease by 30–60 mV when a nonhydrogen-bonding substitution was made at the conserved Thr residue (33,34). Although the disruption of the hydrogen bond to P_A did not alter the rates or relative amplitudes of A_{1B}^- and A_{1A}^- oxidation by F_X (34), the Thr mutations induced a shift of spin-density from P_B toward P_A (33). This result suggests that changes in the strength of the P_A^+ hydrogen bond can alter electronic coupling in the P_{700} dimer, and thus influence the electron-transfer rate from soluble electron carriers to P_{700}^+.

Changes in P_A^+ hydrogen-bond strength may also influence cytochrome/plastocyanin oxidation through structural changes in the protein backbone. Fig. 4 *B* shows the luminal PsaA and PsaB helices in close proximity to P_{700}. This region of PSI was demonstrated to be important in the facilitation of electron transfer from plastocyanin and cytochrome *c* to P_{700}^+ (2,13–15). As suggested in Fig. 4, changes in the angle or distance of the Thr-P_A^+ hydrogen bond are likely to influence the orientation and conformation of these luminal PsaA and PsaB helices. In the cyanobacterium *Synechocystis*, such a change in orientation may alter the rate or mechanism of cytochrome *c* oxidation in vivo (12). For example, it was proposed that a rate-limiting conformation change may occur to regulate oxidation (10,16). A redox-linked conformational change may also regulate the binding affinity of the oxidized and reduced forms of soluble electron carriers (17).

In photosynthetic reaction centers, the protein environment is an inhomogeneous matrix that relaxes after charge separation on many timescales. A complete understanding of photosynthetic electron transfer necessitates a description of these coupled protein conformational changes. To our knowledge, this study provides a new, detailed description of a protein-relaxation event that is coupled to light-induced electron transfer in PSI. We propose that this light-induced change in P_A^+ hydrogen bonding regulates PSI electron transfer reactions.

SUPPLEMENTARY MATERIAL

To view all of the supplemental files associated with this article, visit www.biophysj.org.

The authors thank Dr. L. Gelbaum for assistance with NMR data acquisition, and Prof. Hugo Scheer for helpful discussions.

This work was supported by National Institutes of Health grant GM 43273 (to B.A.B).

REFERENCES

1. Golbeck, J. H., and D. A. Bryant. 1991. Photosystem I. *Curr. Top. Bioenerg.* 16:83–177.
2. Brettel, K., and W. Leibl. 2001. Electron transfer in photosystem I. *Biochim. Biophys. Acta.* 1507:100–114.
3. Jordan, P., P. Fromme, H. T. Witt, O. Klukas, W. Saenger, and N. Krauss. 2001. Three-dimensional structure of cyanobacterial photosystem I at 2.5 Ang resolution. *Nature.* 411:909–917.
4. Joliot, P., and A. Joliot. 1999. In vivo analysis of the electron transfer within photosystem I: are the two phylloquinones involved? *Biochemistry.* 38:11130–11136.
5. Guergova-Kuras, M., B. Boudreaux, A. Joliot, P. Joliot, and K. Redding. 2001. Evidence for two active branches for electron transfer in photosystem I. *Proc. Natl. Acad. Sci. USA.* 98:4437–4442.
6. Holzwarth, A. R., M. G. Muller, J. Niklas, and W. Lubitz. 2006. Ultrafast transient absorption studies on photosystem I reaction centers from *Chlamydomonas reinhardtii*. 2: mutations near the P_{700} reaction center chlorophylls provide new insight into the nature of the primary electron donor. *Biophys. J.* 90:552–565.
7. Webber, A. N., and W. Lubitz. 2001. P_{700}: the primary electron donor of photosystem I. *Biochim. Biophys. Acta.* 1507:61–79.
8. Grotjohann, I., and P. Fromme. 2005. Structure of cyanobacterial photosystem I. *Photosynth. Res.* 85:51–72.
9. Merchant, S., and L. Bogorad. 1986. Regulation by copper of the expression of plastocyanin and cytochrome *c*-552 in *Chlamydomonas reinhardtii*. *Mol. Cell. Biol.* 6:462–469.
10. Bottin, H., and P. Mathis. 1985. Interaction of plastocyanin with the photosystem I reaction center: a kinetic study by flash absorption spectroscopy. *Biochemistry.* 24:6453–6460.
11. Hippler, M., F. Drepper, J. Farah, and J. D. Rochaix. 1997. Fast electron transfer from cytochrome *c*6 and plastocyanin to photosystem I of *Chlamydomonas reinhardtii* requires PsaF. *Biochemistry.* 36: 6343–6349.

12. Durán, R. V., M. Hervás, M. A. De la Rosa, and J. A. Navarro. 2004. The efficient functioning of photosynthesis and respiration in *Synechocystis* sp. PCC 6803 strictly requires the presence of either cytochrome *c*6 or plastocyanin. *J. Biol. Chem.* 279:7229–7233.

13. Sun, J., M. Hervas, J. A. Navarro, M. A. De la Rosa, and P. R. Chitnis. 1999. Oxidizing side of the cyanobacterial photosystem I: mutational analysis of the luminal H loop of the PsaB subunit. *Photosynth. Res.* 62:241–250.

14. Sommer, F., F. Drepper, and M. Hippler. 2002. The luminal helix l of PsaB is essential for recognition of plastocyanin or cytochrome *c*6 and fast electron transfer to photosystem I in *Chlamydomonas reinhardtii*. *J. Biol. Chem.* 277:6573–6581.

15. Sommer, F., F. Drepper, W. Haehnel, and M. Hippler. 2004. The hydrophobic recognition site formed by residues PsaA-Trp651 and PsaB-Trp627 of photosystem I in *Chlamydomonas reinhardtii* confers distinct selectivity for binding of plastocyanin and cytochrome c6. *J. Biol. Chem.* 279:20009–20017.

16. Sigfridsson, K., S. Young, and O. Hansson. 1997. Electron transfer between spinach plastocyanin mutants and photosystem 1. *Eur. J. Biochem.* 245:805–812.

17. Drepper, F., M. Hippler, W. Nitschke, and W. Haehnel. 1996. Binding dynamics and electron transfer between plastocyanin and photosystem I. *Biochemistry.* 35:1282–1295.

18. Breton, J. 2001. Fourier transform infrared spectroscopy of primary electron donors in type I photosynthetic reaction centers. *Biochim. Biophys. Acta.* 1507:180–193.

19. van der Est, A. 2001. Light-induced spin polarization in type I photosynthetic reaction centres. *Biochim. Biophys. Acta.* 1507:212–225.

20. Breton, J., E. Nabedryk, and W. Leibl. 1999. FTIR study of the primary electron donor of photosystem I (P_{700}) revealing delocalization of the charge in P_{700}^{+} and localization of the triplet character in $^{3}P_{700}$. *Biochemistry.* 38:11585–11592.

21. Kaess, H., P. Fromme, H. T. Witt, and W. Lubitz. 2001. Orientation and electronic structure of the primary donor radical cation P_{700}^{+} in photosystem I: a single crystal EPR and ENDOR study. *J. Phys. Chem. B.* 105:1225–1239.

22. Wang, H., S. Lin, J. P. Allen, J. C. Williams, S. Blankert, C. Laser, and N. W. Woodbury. 2007. Protein dynamics control the kinetics of initial electron transfer in photosynthesis. *Science.* 316:747–750.

23. Warshel, A., Z. T. Chu, and W. W. Parson. 1989. Dispersed polaron simulations of electron transfer in photosynthetic reaction centers. *Science.* 246:112–116.

24. Gehlen, J. N., M. Marchi, and D. Chandler. 1994. Dynamics affecting the primary charge transfer in photosynthesis. *Science.* 263:499–502.

25. Parson, W. W., and A. Warshel. 2004. Dependence of photosynthetic electron-transfer kinetics on temperature and energy in a density-matrix model. *J. Phys. Chem. B.* 108:10474–10483.

26. Halverson, K. M., and B. A. Barry. 2003. Evidence for spontaneous structural changes in a dark-adapted state of photosystem II. *Biophys. J.* 85:2581–2588.

27. De Riso, A., D. L. Jenson, and B. A. Barry. 2006. Calcium exchange and structural changes during the photosynthetic oxygen evolving cycle. *Biophys. J.* 91:1999–2008.

28. Barry, B. A., I. Cooper, A. De Riso, S. H. Brewer, D. M. Vu, and R. B. Dyer. 2006. Time-resolved vibrational spectroscopy detects protein-based intermediates in the photosynthetic oxygen-evolving cycle. *Proc. Natl. Acad. Sci. USA.* 103:7288–7291.

29. Kim, S., and B. A. Barry. 2000. Identification of carbonyl modes of P_{700} and P_{700}^{+} by in situ chlorophyll labeling in photosystem I. *J. Am. Chem. Soc.* 122:4980–4981.

30. Nabedryk, E., M. Leonhard, W. Maentele, and J. Breton. 1990. Fourier transform infrared difference spectroscopy shows no evidence for an enolization of chlorophyll *a* upon cation formation either in vitro or during P_{700} photooxidation. *Biochemistry.* 29:3242–3247.

31. Hastings, G., V. M. Ramesh, R. Wang, V. Sivakumar, and A. Webber. 2001. Primary donor photo-oxidation in photosystem I: a re-evaluation of (P_{700}^{+} $-P_{700}$) Fourier transform infrared difference spectra. *Biochemistry.* 40:12943–12949.

32. Bellamy, L. J. 1980. Advances in Infrared Group Frequencies: The Infrared Spectra of Complex Molecules. Chapman and Hall, New York. 263–275.

33. Witt, H., C. Teuloff, J. Niklas, E. Bordignon, D. Carbonera, S. Kohler, A. Labahn, and W. Lubitz. 2002. Hydrogen bonding of P_{700}: site-directed mutagenesis of threonine A739 of photosystem I in *Chlamydomonas reinhardtii*. *Biochemistry.* 41:8557–8569.

34. Li, Y., M. G. Lucas, T. Konovalova, B. Abbott, F. MacMillan, A. Petronko, V. Sivakumar, R. Wang, G. Hastings, F. Gu, J. van Tol, L. C. Brunal, R. Timkovich, F. Rappaport, and K. Redding. 2004. Mutation of the putative hydrogen-bond donor to P_{700} of photosystem I. *Biochemistry.* 43:12634–12647.

35. Pantelidou, M., P. R. Chitnis, and J. Breton. 2004. FTIR spectroscopy of *Synechocystis* 6803 mutants effected on the hydrogen bonds to the carbonyl groups of the PsaA chlorophyll of P_{700} supports an extensive delocalization of the charge in P_{700}^{+}. *Biochemistry.* 43:8380–8390.

36. Beale, S. I. 1999. Enzymes of chlorophyll biosynthesis. *Photosynth. Res.* 60:43–73.

37. Porra, R. J., and H. Scheer. 2001. ^{18}O and mass spectrometry in chlorophyll research: derivation and loss of oxygen atoms at the periphery of the chlorophyll macrocycle during biosynthesis, degradation and adaptation. *Photosynth. Res.* 66:159–175.

38. Rippka, R., J. Deruelles, J. B. Waterbury, M. Herdman, and R. Y. Stanier. 1979. Generic assignments, strain histories and properties of pure cultures of cyanobacteria. *J. Gen. Microbiol.* 111:1–61.

39. Barry, B. A. 1995. Tyrosyl radicals in photosystem II. *Methods Enzymol.* 258:303–319.

40. Noren, G. H., R. J. Boerner, and B. A. Barry. 1991. EPR characterization of an oxygen-evolving photosystem II preparation from the transformable cyanobacteria *Synechocystis* 6803. *Biochemistry.* 30:3943–3950.

41. Kim, S., C. A. Sacksteder, K. A. Bixby, and B. A. Barry. 2001. A reaction-induced FT-IR study of cyanobacterial photosystem I. *Biochemistry.* 40:15384–15395.

42. Sacksteder, C. A., S. L. Bender, and B. A. Barry. 2005. Role for bound water and CH-pi aromatic interactions in photosynthetic electron transfer. *J. Am. Chem. Soc.* 127:7879–7890.

43. Bender, S. L., J. Keough, S. E. Boesch, R. A. Wheeler, and B. A. Barry. 2008. The vibrational spectrum of the secondary electron acceptor, A_1, in photosystem I. *J. Phys. Chem. B.* 112:3844–3852.

44. Wong, Y. S., P. A. Castelfranco, D. A. Goff, and K. M. Smith. 1985. Intermediates in the formation of the chlorophyll isocyclic ring. *Plant Physiol.* 79:725–729.

45. Walker, C. J., K. E. Mansfield, K. M. Smith, and P. A. Castelfranco. 1989. Incorporation of atmospheric oxygen into the carbonyl functionality of the protochlorophyllide isocyclic ring. *Biochem. J.* 257: 599–602.

46. Schneegurt, M. A., and S. I. Beale. 1992. Origin of the chlorophyll b formyl oxygen in *Chlorella vulgaris*. *Biochemistry.* 31:11677–11683.

47. Bollivar, D. W., and S. I. Beale. 1995. Formation of the isocyclic ring of chlorophyll by isolated *Chlamydomonas reinhardtii* chloroplasts. *Photosynth. Res.* 43:113–124.

48. Bollivar, D. W., and S. I. Beale. 1996. The chlorophyll biosynthetic enzyme Mg-protoporphyrin IX monomethyl ester (oxidative) cyclase. Characterization and partial purification from *Chlamydomonas reinhardtii* and *Synechocystis* sp. PCC 6803. *Plant Physiol.* 112:105–114.

49. Beale, S. I., S. P. Gough, and S. Granik. 1975. Biosynthesis of delta-aminolevulinic acid from the intact carbon skeleton of glutamic acid in greening barley. *Proc. Natl. Acad. Sci. USA.* 72:2719–2723.

50. Porra, R. J., O. Klein, and P. E. Wright. 1983. The proof by ^{13}C-NMR spectroscopy of the predominance of the C5 pathway over the Shemin pathway in chlorophyll biosynthesis in higher plants and of the formation of the methyl ester group of chlorophyll from glycine. *Eur. J. Biochem.* 130:509–516.

51. Huang, D. D., and W. Y. Wang. 1986. Chlorophyll biosynthesis in *Chlamydomonas* starts with the formation of glutamyl-tRNA. *J. Biol. Chem.* 261:13451–13455.

52. Schön, A., G. Krupp, S. Gough, S. Berry-Lowe, C. G. Kannangara, and D. Söll. 1986. The RNA required in the first step of chlorophyll biosynthesis is a chloroplast glutamate tRNA. *Nature.* 322:281–284.

53. Rieble, S., and S. I. Beale. 1988. Transformation of glutamate to delta-aminolevulinic acid by soluble extracts of *Synechocystis* sp. PCC 6803 and other oxygenic prokaryotes. *J. Biol. Chem.* 263:8864–8871.

54. Boldt, N. J., R. J. Donohoe, R. R. Birge, and D. F. Bocian. 1987. Chlorophyll model compounds: effects of low symmetry on the resonance Raman spectra and normal mode descriptions of nickel (II) dihydroporphyrins. *J. Am. Chem. Soc.* 109:2284–2298.

55. Sachs, R. K., K. M. Halverson, and B. A. Barry. 2003. Specific isotopic labeling and photooxidation-linked structural changes in the manganese-stabilizing subunit of photosystem II. *J. Biol. Chem.* 278:44222–44229.

56. Patzlaff, J. S., and B. A. Barry. 1996. Pigment quantitation and analysis by HPLC reverse phase chromatography: a characterization of antenna size in oxygen-evolving photosystem II preparations from cyanobacteria and plants. *Biochemistry.* 35:7802–7811.

57. Breton, J., P. R. Chitnis, and M. Pantelidou. 2005. Evidence for hydrogen bond formation to the PsaB chlorophyll of P_{700} in photosystem I mutants of *Synechocystis* sp. PCC 6803. *Biochemistry.* 44: 5402–5408.

58. Xu, W., P. Chitnis, A. Valieva, A. van der Est, Y. N. Pushkar, M. Krzystyniak, C. Teutloff, S. G. Zech, R. Bittl, D. Stehlik, B. Zybailov, G. Shen, and J. H. Golbeck. 2003. Electron transfer in cyanobacterial photosystem I: I. Physiological and spectroscopic characterization of site-directed mutants in a putative electron transfer pathway from A_0 through A_1 to F_x. *J. Biol. Chem.* 278:27864–27875.

59. Xu, W., P. R. Chitnis, A. Valieva, A. van der Est, K. Brettel, M. Guergova-Kuras, Y. N. Pushkar, S. G. Zech, D. Stehlik, G. Shen, B. Zybailov, and J. H. Golbeck. 2003. Electron transfer in cyanobacterial photosystem I: II. Determination of forward electron transfer rates of site-directed mutants in a putative electron transfer pathway from A_0 through A_1 to F_x. *J. Biol. Chem.* 278:27876–27887.

60. Heller, B. A., D. Holten, and C. Kirmaier. 1995. Control of electron-transfer between the L- and M-sides of photosynthetic reaction centers. *Science.* 269:940–945.

61. Kirmaier, C., D. Weems, and D. Holten. 1999. M-side electron transfer in reaction center mutants with a lysine near the nonphotoactive bacteriochlorophyll. *Biochemistry.* 38:11516–11530.